New approach for coupled chloride/moisture transport in non-saturated concrete with and without slag

Amor Ben Fraj, Stéphanie Bonnet, Abdelhafid Khelidj

New approach for coupled chloride/moisture transport in non-saturated concrete with and without slag

Amor Ben Fraj [a,*], Stéphanie Bonnet [b], Abdelhafid Khelidj [b]

[a] CETE IdF, Laboratoire Eco-matériaux, Le Bourget, France
[b] LUNAM Université, Université de Nantes – IUT Saint-Nazaire, GeM, CNRS UMR 6183, Institut de Recherche en Génie Civil et Mécanique, France

Over the paste decades a considerable research effort has been attributed to chloride ingress into reinforced concrete in order to understand the transport mechanisms and to predict its durability.

In saturated concrete, chloride ions enter through diffusion (concentration gradient), whereas in partially saturated concrete, a part of the invading chloride is transported along with the salty water that was sucked by capillary absorption into the dried concrete. This study examines the effects of cyclic drying and wetting with chloride sodium on chloride ingress into non-saturated concrete. For this aim, a new automatic experimental setup has been developed to apply cyclic movement of chloride solution in controlled environmental conditions ambiance. Likewise, a new astute test method to control the concrete moisture content has been presented. As results, the first part of our study concerns chloride binding and water vapour adsorption isotherms. Results showed that Blast Furnace Slag (BFS), used as partial substitution of cement, increases the performances of concrete (BFSC60). Furthermore, the interaction chloride/concrete matrix seems to increase the adsorbed water vapour. In the second part of this research work, the influence of the moisture content, the number of cycles, the water-to-binder ratio and the slag's addition on chloride profiles has been investigated and analysed. The results showed that the decreasing of relative humidity from 90% to 50% enabled to increase by ≈2–9 times the apparent chloride diffusion coefficient, which decreased when the number of cycles increased. A correlation between apparent diffusion coefficient and relative humidity has been obtained.

1. Introduction and scientific background

Durability aspects are increasingly decisive for the design of reinforced concrete structures in aggressive environment (e.g., structures exposed to seawater or deicing salts). Except in submerged parts of marine structures, concrete is rarely saturated when exposed to chlorides. Therefore, studies of chloride ingress into partially saturated concrete are relevant for the service life design and reassessment of reinforced concrete structures.

According to environmental conditions, which concrete structures undergo in a saline ambiance, different and simultaneous mechanisms of chloride ingress could operate [1]. In the case of sea-immersed structures, considered as water-saturated concrete, pure diffusion seems to be the only mechanism operating in chloride ingress [2]. However, in tidal zone, concrete was subjected to cyclic wetting and drying, coupling vapour and liquid movements. This phenomenon induced a non-saturated state of concrete and an inhomogeneous spatial distribution of moisture within concrete [3]. In these environmental conditions, diffusion of chlorides operates simultaneously with capillary absorption of salty water [4]. This process is known to cause faster penetration of chloride [5]. Furthermore, cyclic movement of salty water may

* Corresponding author. Tel.: +33 1 48 38 81 09; fax: +33 1 48 38 81 01.
E-mail address: amor.ben-fraj@developpement-durable.gouv.fr (A. Ben Fraj).

lead to accumulation of chloride, as the salt remains in the concrete after evaporation of the absorbed water and exhibits alternating moisture content. This phenomenon increases capillary suction [6] and the "availability of oxygen required for steel corrosion" [5]. Thus, concrete structures subjected to cyclic wetting and drying of seawater are more prone to corrosion–deterioration compared to concrete structures permanently submerged in seawater [7].

Since chloride and oxygen penetration into non-saturated concrete is paramount to corrosion initiation, many authors [8–18] have focused on understanding and modelling this phenomenon. Particularly, Saetta et al. [8], Ababneh et al. [12] and Meijers et al. [14] proposed various models, taking into account the dependence on environmental conditions and concrete mix parameters, for chloride ingress in unsaturated concrete. Recently, Bastidas-Arteaga et al. [18] proposed a comprehensive probabilistic model, which considers the uncertainties related to the phenomenon by including the influence of random nature of environmental actions, chloride binding, convection and two-dimensional chloride ingress. Although numerical models were developing, experimental studies on chloride ingress in non-saturated concrete are not still realistic and do not take into account all environmental conditions of structures in tidal zone.

In 2002, Climent et al. [19] proposed a test method for measuring chloride diffusion coefficients through non-saturated concrete. In this research work, concrete specimens were dried at 50 °C for 1, 3 and 5 days. Then they were kept in corresponding climatic chamber conditioning at relative humidity (RH) 86%, 75% and 54% and 20 °C for at least three weeks. The chloride contamination of these specimens was by gaseous hydrogen chloride produced by PVC combustion and continuously. There were no wetting–drying cycles. Authors have measured more chlorides for concrete with higher moisture content (86%), after 180 days of chloride contamination. Meijers et al. [14], have compared their numerical results to experimental results of Taheri-Motlagh [20]. In this research work ([20], cited in [14]), concrete beams were subjected to cyclic exposure of 6 h wetting with 50 g/l of NaCl solution and 42 h drying. The experiments were performed at constant temperature of 20 °C and at sinusoidal temperature variations between 20 °C and 60 °C during the drying phases (and constant at 20 °C during the wetting phases). However, the air humidity was not controlled during drying phases. The initial moisture of samples was fixed at 95%. Authors have only drawn chloride profiles and did not compare different initial moisture contents.Bhattacharjee and Nagesh [9] compared numerical and experimental profiles of saturated and unsaturated concretes. Before testing, unsaturated concrete was completely oven dried. Further, all prismatic specimens were wrapped with polythene sheets to avoid evaporation, except one face, which will be exposed to chloride solution. Saturated and unsaturated concretes were exposed continuously to NaCl solution of 30 g/l. Chloride diffusion coefficients were calculated with Boltzman transformation, for 24 h and 120 h of chloride exposure. The diffusion coefficient of dried concrete was 26 times more than for saturated one.

Among the works concerning chloride transport in non-saturated concrete, it is important to highlight the experimental study carried out by Hong and Hooton [5]. This study performed some real conditions by applying wetting/drying cycles that concrete structures could undergo. Specimens were sealed on all sides except for the testing surface and then exposed to 60 g/l of NaCl solution. The wetting period was kept constant for 6 h and the drying was 18 h. This 1-day cycle represents daily application of deicing salts during a Canadian winter. As the rate of drying is slower than the rate of wetting, the drying time was set at 18 h. However, cycles are applied by moving manually the specimen from drying chamber to wetting container. Indeed, wetting and drying were applied in two different chambers, which could disturb environmental conditions and hygral state of concrete samples, when moving them. Besides, the air humidity (50%) in drying chamber was controlled by saturated salt solution ($CaCl_2$), which could disturb ambiance humidity by interaction with concrete specimens.

For monitoring the cover concrete depth, some authors [21,22] proposed humidity and temperature sensors, but any one have succeed in monitoring coupled transport of chloride and moisture in concrete by measuring all parameters. As non-destructive techniques are not available to determine chloride profiles in concrete, these were performed by destructive method in this study.

2. Research aim

Within this context, this paper presents an experimental study on chloride ingress into non-saturated concrete in realistic conditions by controlling temperature (called *T*) and relative humidity (called RH). The purpose was to analyse the influence of:

- Time exposure and environmental conditions (RH and *T*).
- Concrete composition: water-to-binder ratio and the slag's addition.

on chloride profiles and chloride coefficient transport deduced from them.

The originality of the present work lies in the new automatic experimental setup developed in order to apply cyclic tests in controlled environmental conditions. This work was performed to understand the physical mechanisms governing chloride ingress into concrete during the wetting and drying phases of the cycle. Moisture content was measured during the test, using capacitive probes placed in concrete specimens.

A comparison between chloride profiles of submerged specimens (NT BLUID 443) and specimens subjected to wetting/drying cycles was presented. Moreover the moisture adsorption isotherm tests were performed with concretes contaminated with chloride. These studies were done to understand the transport phenomena in non-saturated concrete in contact with chloride solution.

The effects of the number of cycles and the moisture content on chloride ingress in three different concretes mixtures are discussed. The effects of mixture parameters and chloride contamination on chloride binding and water vapour adsorption isotherms, on transfer and physical parameters were also presented and discussed.

3. Experimental study

3.1. Materials

The cement used is an ordinary Portland cement CEM I 52.5N PM ES from Le Havre (France). Its chemical composition and main physico-chemical properties are detailed in Table 1.

The Blast Furnace Slag (BFS) is from Moerdijk (Netherlands). Its chemical composition is detailed in Table 1.

The sand is a calcareous 0/4 mm sand with a specific gravity of 2650 kg/m^3 and a water absorption coefficient of 0.77% (in mass). The coarse aggregates are calcareous gravels 4/12 mm and 12/20 mm (specific gravity: 2670 kg/m^3 and water absorption coefficient: 0.7%, in mass).

A polycarboxylate-based superplasticizer (SP) was added to the concretes with lower water-to-binder-ratio in order to reduce the amount of mixing water needed. In liquid form, it has a specific gravity of 1070 kg/m^3 and a dry content of 20%.

3.2. Concrete mixtures

For this study, cylindrical concrete specimens, 22 cm in height and 11 cm in diameter, were cast following three dosages given in Table 2. These concretes are designated: OPCC30, an ordinary Portland cement concrete with a water-to-binder ratio (W/B) of 0.7; OPCC60 and BFSC60, both similar concretes with a W/B of 0.48, except that one contains BFS.

Table 1
Chemical composition of cement and slag.

Compounds	% (by weight)	
	Cement	Slag
CaO	64.95	41.03
SiO2	21.25	34.49
Al2O3	3.47	13.19
Fe2O3	4.23	0.4
MgO	0.96	8.21
K2O	0.28	0.54
Na2O	0.10	0.43
SO3	2.63	0.1
Specific surface (m^2/kg)	382	462
Density (–)	3.18	2.89
Main compounds (Bogue's equation)% by weight		
C3S	67.5	–
C2S	10.7	–
C3A	2.64	–
C4AF	12.8	–
Gypsum	3.3	–

Table 2
Concrete mixtures.

Constituents (kg/m^3)	OPCC30	OPCC60	BFSC60
Coarse aggregate, 12–20 mm	563.4	561.2	561.2
Medium aggregate, 4–12 mm	433.7	432	432
Sand (Boulonnais), 0–4 mm	903.5	867.8	867.8
Cement CEM I 52.5 N PM ES	260	350	242.9
Slag	–	–	104.1
Superplasticizer	–	3	3
Water	182	168	166.6
Water-to-binder ratio (W/B)	0.7	0.48	0.48

OPCC30 (W/B = 0.7) and OPCC60 (W/B = 0.48) were chosen to show the effect of W/B on chloride profiles and diffusion coefficient. The influence of BFS on chloride transport was evaluated by comparing OPCC60 with BFSC60. These both concretes are used for marine reinforced concrete structures in France [23].

3.3. Experimental steps

Fig. 1 described the experimental procedure. Some 110 × 220 mm cylindrical samples were prepared from a single batch for each mix. The concrete mixtures were cast in steel moulds and compacted using a mechanical vibrator. The specimens were moist-cured at 20 ± 2 °C and over 95 ± 5% of relative humidity for 24 h. They were kept in a water tank at 20 ± 2 °C for 3 months.

Concrete cylinders were cut using a diamond blade saw to obtain 50 mm-thick discs. Their curved surface was sealed with two epoxy resin layers to ensure a one-dimensional flow inside the discs and polished to have plane and cleaned surfaces. Some discs were oven-dried at 60 °C until reaching constant weight [24]. Then they were cooled for 48 h in a desiccator at 20 °C before being tested to evaluate gas permeability. After permeability evaluation the specimens are saturated [25] to determine their water porosity and their effective chloride diffusion coefficient.

The first parameter was determined using a Cembureau constant head permeameter [25,26] and the second one, using the steady state migration test [27]. The properties of concrete mixes: Mechanical properties, water porosity, gas permeability and effective chloride migration coefficient, are summarised in Table 3. The values provided are the average values obtained from three experimental results.

Some 50 mm-thick discs were used for drying wetting cycles and other were crushed to determine chloride binding and moisture adsorption isotherms.

3.4. Chloride binding isotherms

The equilibrium procedure, proposed in [28] and based on the method of Tang and Nilsson [29], to establish chloride-binding isotherms was followed in this work.

After crushing the 5-cm discs, samples were sieved and only the part with a diameter within the range 0.25–2 mm is conserved [28] and then oven-dried at 40 °C. After drying, 100 g samples were stored in plastic boxes. The boxes were filled with a known volume (400 ml) of NaCl solutions of varying initial concentrations called C_0 (3, 15, 30, 60, 90, 120 g/l of NaCl). NaOH (1 g/l) and KOH (4.65 g/l) were added to the chloride solutions to avoid leaching. The boxes were sealed and stored in the laboratory atmosphere with controlled temperature (20 °C) for 2–3 months to allow equilibrium to be established. Then, knowing the initial and final concentration, the volume of the external solution and the dry mass of the sample, the amount of bound chloride can be calculated according to the following equation [29]:

$$c_b = \frac{35,453V(c_0 - c_f)}{m} \quad (1)$$

where c_b is the amount of bound chloride in g Cl^-/g of sample; V is the volume of the external solution in l; c_0 is the initial chloride concentration of the external solution in mol/l; c_f is the free chloride concentration at equilibrium of the external solution in mol/l; m is the dry mass of the sample in g and 35.453 is the molar mass of the chloride ion in g/mol.

Solutions were titrated by means of potentiometric titration versus 0.05 M $AgNO_3$ titrant with a silver electrode.

3.5. Water vapour adsorption isotherms

The water vapour sorption isotherm is used to understand and quantify the hygral behaviour of hardened cementitious material [30]. The curve, water content (w) versus relative humidity (RH), quantifies the water–solid interactions at the origin of durability properties [31], particularly in non-saturated materials where the moisture transport is an important mechanism. Various methods can be used for the assessment of water vapour sorption isotherms [30]. The gravimetric method, where adsorption experiments have been performed by means of saturated salt

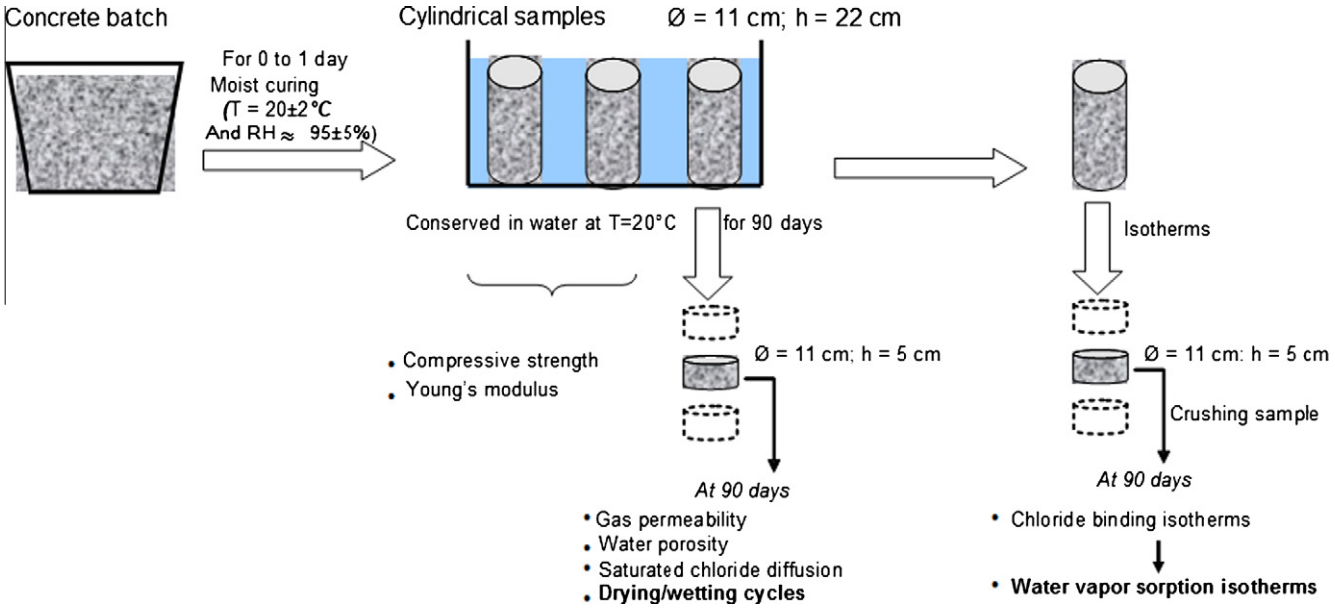

Fig. 1. Experimental steps of research work.

Table 3
Concrete properties.

	OPCC30	OPCC60	BFSC60
90-Day water porosity (%)	13	10.21	9.73
28-Day compressive strength (MPa)	38.2	66.7	60.2
90-Day compressive strength (MPa)	48.6	74.7	81.6
90-Day intrinsic permeability (m^2)	1.2×10^{-17}	0.76×10^{-17}	0.34×10^{-17}
90-Day chloride migration coefficient (m^2/s)	6.04×10^{-12}	2.8×10^{-12}	0.96×10^{-12}

solutions, is the most used. It consists in enclosing the specimens in sealed cells, where the relative humidity is kept constant by means of saturated salt solution, and then evaluating their equilibrium mass water content (water mass/sample dry mass).

The originality of this study is that samples were firstly chloride-contaminated to simulate real conditions and to study the effect of chlorides on water vapour adsorption of concrete. Samples were contaminated with chloride solutions (§ 3.4) of 30, 60 and 120 g/l of NaCl. After their chloride saturation to establish chloride binding isotherms, samples were filtered and oven dried at 40 °C. Then, 6 g specimens (for every external chloride solution and every concrete) were put in open plastic containers, which would be conserved in a sealed cell (40 × 50 × 15 cm) with controlled humidity (Fig. 2). To control the homogeneity of the humidity in every cell, a capacitive probe was placed in its upper part. We supposed that there was not a RH gradient in the cell. In Table 4 we show the difference between the theoretical and measured humidities. Two reasons could explain this difference:

- For a temperature of 20 °C, it is difficult to obtain a relative humidity closed to 100% because of the high moisture content required.
- The high volume of the cell and probably the small quantity of saturated solution (1.25 l), used for high ambiance's humidities.

3.6. Wetting/drying cycle

3.6.1. Experimental setup

An experimental setup was developed (Fig. 3) to monitor automatically the wetting and drying cycles in controlled ambiance ($T°$, HR). The cycles are applied on concrete specimens in the immersion tank, which is in a climatic chamber. This chamber was adapted for this experience: the lateral parts were reinforced to support the immersion tank filled with concrete specimens and chloride solution. This chamber was also perforated for:

- Tubes to fill and empty the tank with chloride solution.
- Data acquisition connections: the capacitive probes (RH and T) are linked to the data monitor.
- Connections to monitor electrical valve and pump: these are used to fill and empty the tank.

A program was implemented in the computer connected to the data monitor to drive the wetting and drying cycles and to register the data.

The voids between perforated holes and connections were sealed to maintain RH and Temperature in climatic chamber.

The chloride solution is stored in a container, which is outside of the climatic chamber and the solution level in the immersion tank was controlled by an overflow.

3.6.2. Preconditioning of samples

The relative humidities (RH) applied on concrete specimens in climatic chamber were 50% (summer conditions), 75% (frequent relative humidity) and 90% (winter raining conditions). The specimens were preconditioned after curing and before exposure to drying–wetting cycles to get these RH inside:

- For RH of 90% the specimens were kept in the curing chamber.
- For RH of 50% and 75% the specimens (5 cm discs) were dried [19] with the procedure described in Fig. 4. A cylindrical specimen (diameter: 11 cm; height: 22 cm), with some holes (diameter: 6 mm; depth inside concrete: 5 cm) was oven dried progressively at 80 °C and its relative humidity was measured using a capacitive probe (Figs. 5). When the chosen relative humidity is reached (±3%), the water content of specimen was determined by weighing. Then 5 cm-discs were dried and weighed until reaching the water content corresponding to the fixed relative humidity. The drying duration depends on the concrete water-to-binder-ratio and the fixed relative humidity of the ambiance.

3.6.3. Testing program

When RH was reached, concrete samples were sealed except on the surface, which is in contact with chloride solution called testing surface to get a one-dimensional transport. The disc height (5 cm) is corresponding to concrete cover depth for marine reinforced structures. The opposite surface of testing surface was sealed to simulate chloride transport in this cover concrete where only one face is in environmental conditions. They were then placed in the immersion tank.

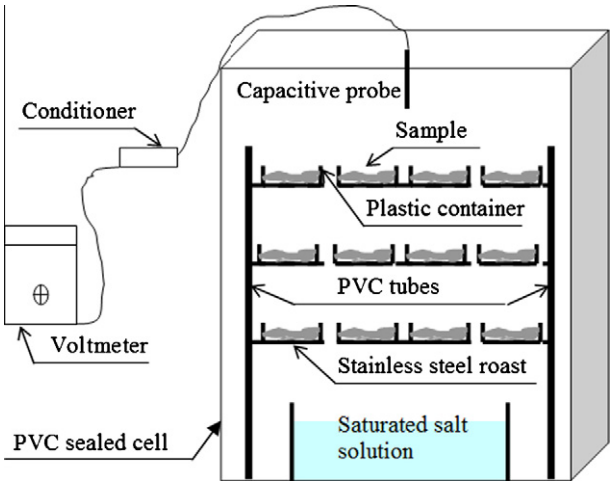

Fig. 2. Developed experimental setup for water-vapour-adsorption isotherm.

Table 4
Theoretical and experimental Relative humidities of saturated salt solutions.

Saturated salt solution	Comparison of Relative Humidities obtained at 20 °C	
	Theory	Experiment
Lithium chloride	12	12
Magnesium nitrate	55	53
Ammonium nitrate	65	62
Sodium chloride	76	73
Potassium chloride	86	80
Potassium sulphate	97	90

For each kind of concrete used in test, a cylindrical specimen of 22 cm height was also placed in the climatic chamber. These specimens were sealed on all surfaces except on the testing one. As shown in Fig. 6, capacitive probes were embedded in concrete, at different heights, to control pores' RH, during wetting/drying cycles.

Concrete samples were subjected to cyclic exposure consisting of 6 h wetting periods with 30 g/l NaCl solution, and 6 h drying periods. This cycle was chosen to represent daily application of salts that a reinforced concrete structure might undergo in a tidal zone. The experiments were performed in the climatic chamber at constant temperature 20 °C and three air relative humidities 50%; 75% and 90%.

The specimens were subjected to 2, 10, 20 and 60 wetting/drying cycles (1, 5, 10 and 30 days) of chloride solution and then their chloride profiles were determined and analysed.

3.6.4. Total chloride profiles: determination and analysis

After exposure of the specimens, cylindrical cores were taken from the immersion tank to be ground in 2 or 3-mm thick layers, perpendicular to the testing surface, using a grinding instrument. The powder was collected and stored in sealed plastic bags. A 5-g-sample was taken from each layer of powdered concrete and placed in a 250 cm^3 beaker. HNO_3 and deionized water were added and the mixture was stirred and heated to 80 °C for 30 min [28]. This solution was filtered into a 250 cm^3 volumetric flash.

The chloride concentration of these filtered solutions was determined by potentiometric titration with an automatic titrator using 0.05 M silver nitrate ($AgNO_3$) titrant.

When chloride profiles are established, the surface chloride content C_s and the apparent diffusion coefficient, D_a, could be calculated by fitting the experimental data profiles to Eq. (2), solution of second Fick's law [32]:

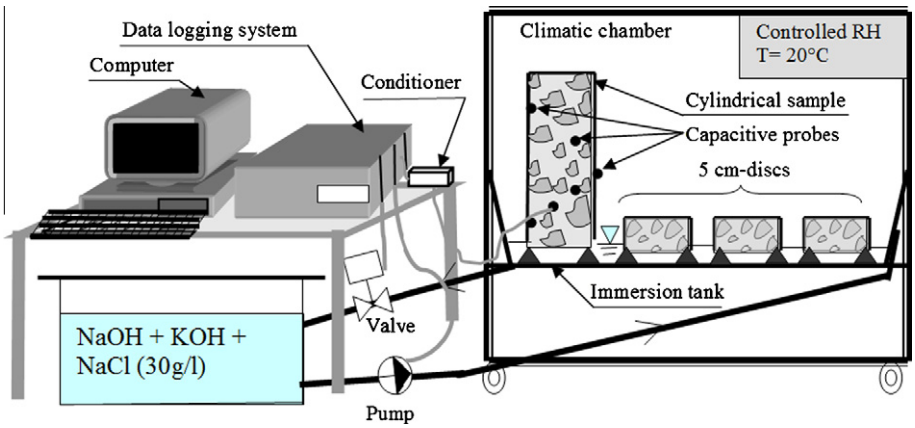

Fig. 3. Developed experimental setup for wetting–drying cycles.

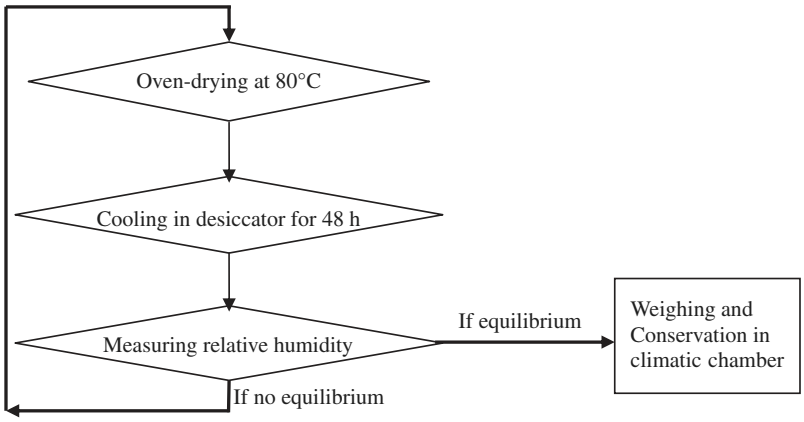

Fig. 4. Test method on cylinder of 22 cm height for determining water content corresponding to the fixed relative humidity.

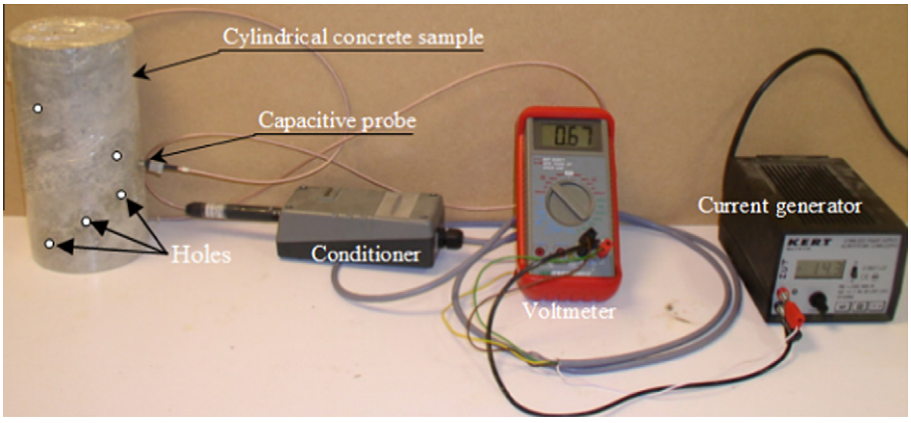

Fig. 5. Measuring relative humidity.

$$C(x,t) = C_s - (C_s - C_i).erf\frac{x}{\sqrt{4.D_a.t}} \quad (2)$$

where $C(x,t)$ is the total chloride content at a depth x (m) and exposure time t (s); C_s (g of chloride/g of material) is the chloride content at the surface; C_i (g of chloride/g of material) is the total background chloride content (considering to be zero in this study) and D_a (m^2/s) is the apparent diffusion coefficient.

This particular solution of second Fick's law of diffusion, corresponds to the instantaneous plane source case in a semi-infinite medium [32] and is used to fit experimental chloride profile when these are decreasing.

4. Results and discussion

The results summarised in Table 3 are in agreement with previous studies [33] that show a decreasing of porosity, gas permeability and chloride diffusion coefficient and an increasing of compressive strength when W/B decreases from 0.7 to 0.48.

As shown, the partially substitution of cement by BFS has beneficial effects on concrete properties. By comparing properties of OPCC60 (reference properties value) and BFSC60 at 90 days, poros-

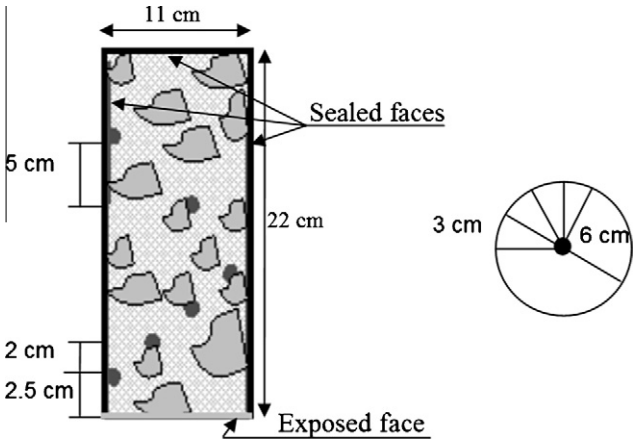

Fig. 6. Vertical (on the left) and radial (on the right) capacitive probes placement.

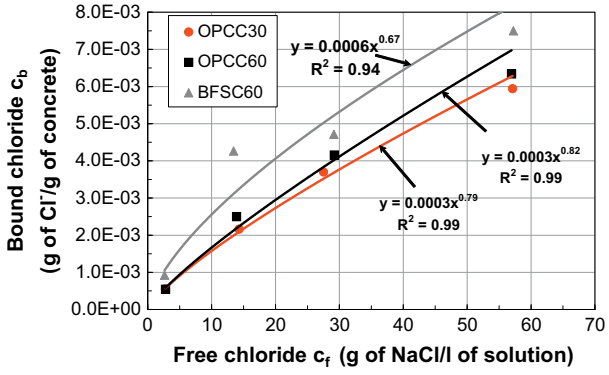

Fig. 7. Chloride binding isotherms.

ity decreases by 5% and compressive strength increases by 9% when BFS is added. Otherwise, the incorporation of this mineral addition (BFS) decreases by two and three times, gas permeability and chloride diffusion, respectively.

4.1. Chloride binding

A comparison of chloride binding isotherms of three concretes was given in Fig. 7, where each curve represents the average of two experimental results (standard deviation < ±9%). These results show that BFSC60 and OPCC60 have the higher amount of bound chloride. These results agreed with those of Hirao et al. [34], who attributed this binding capacity to the formation of Friedel's salt.

The partial substitution of cement by BFS increases the chloride binding capacity: for instance bound chlorides content is 13% higher for BFSC60 than for OPCC60 at 30 g/l of NaCl. This higher binding capacity may be due to the high alumina content in slag. Many researchers [35,36] have shown the same trends. Xu [37] ascribed the higher binding capacity of cement-slag to the dilution effects of sulphate ions, when cement pastes are admixed with chloride solution.

The binding isotherm fits well to a Freundlich-type adsorption with correlation coefficient close to 1 except for BFSC60: the bound chloride content for C_0 = 15 g/l does not fit with Freundlich equation. By removing this value the correlation will be closed to 1.Yuan et al. [38] have reported that the Freundlich equation fits the data very well in a range of free chloride concentrations from 0.5 to 60 g/l (of NaCl). Truc [39] used Freundlich binding isotherm to model forecast the chloride ingress into concrete.

4.2. Water vapour adsorption

4.2.1. Equilibrium state and kinetic aspect

Equilibrium state is considered when the external RH is equal to the internal one, as the material is in thermodynamical equilibrium with its environment. For cementitious materials, this state is not reached before several months. It is therefore necessary to take into account the very slow kinetics for these porous media, where the transport process is further slowed down by:

- Water–matrix interactions.
- Chloride–matrix interactions: the specimens were exposed to salt solution and not pure water.

So the transport is controlled by Darcy's and Fick's law, respectively for the liquid phases and the water vapour diffusion inside the material.

The curves, presented in Fig. 8, are the average of two experimental results. They show the slow evolution of water content versus time, for the concretes without chloride, and for 73% of RH (theoretical initial RH = 76%). After 110 days, the water content seems to be stabilized for several weeks and this content is the equilibrium water content for 73% of RH, which is used for isotherm curves.

4.2.2. Water vapour adsorption isotherms

4.2.2.1. Comparison between different materials. Fig. 9 shows the influence of mix parameters on the equilibrium moisture properties. It can be seen that a low W/B and the partial substitution of cement by slag reduce the equilibrium water content of concrete. Baroghel-Bouny et al. [40] have pointed out the effect of these parameters, "*inducing a very narrow pore network*", on the moisture properties of hardened concrete. They shown a very small water content variations for Relative Humidity running between RH = 50% and RH = 90%. In our case, the lowest W/B is of 0.48, so the difference between concretes, concerns specially the value of equilibrium water content and not the variation rate (curve shape).

This result is very interesting to understand the chloride ingress in non-saturated concrete. Indeed, the lowest porous concretes (with the lowest W/B and with slag) are less sensitive to environmental (moisture) conditions and the moisture transport is slower in these concretes. This process can influence chloride transfer and its penetration depth, as it will be discussed later (§ 4.3).

4.2.2.2. Effect of chloride contamination on water vapour adsorption isotherms. In this section, the influence of chloride contamination (chloride/matrix interaction) on the equilibrium moisture properties is investigated. Fig. 10a–c shows the water vapour adsorption isotherms of concretes contaminated with chloride (§ 3.4). For the relative humidity of 93%, water content is very high, especially for

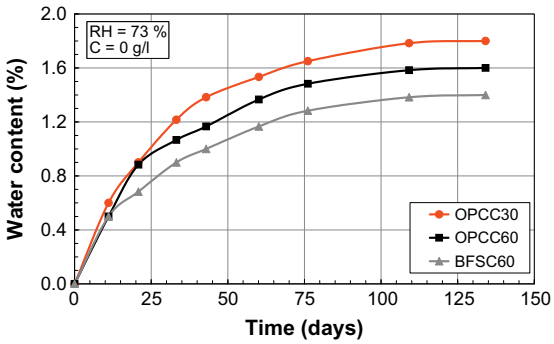

Fig. 8. Water adsorption kinetic.

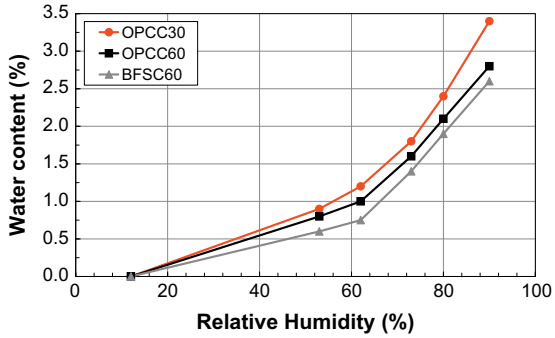

Fig. 9. Water vapour adsorption isotherms for C = 0 g/l of NaCl.

samples contaminated with 120 g/l chloride solution. This is due to the condensation of water on the surface of concrete aggregates, which was observed visually. Indeed, the checked sample's mass did not represent only saturated aggregates but also the exceed water, present in the plastic container (Fig. 2). Thus, the water content was over-estimated.

As it can be observed for all cases, equilibrium water content increases with the chloride concentration. This could be explained by the modification of water activity coefficient [41], which is due to the presence of salt and other ions (Na^+,K^+...). Indeed, the liquid/vapour equilibrium is reached for RH ≈ 100% for the case of pure water. This equilibrium was reached for RH ≈ 76% for an entirely saturated chloride solution. If we took the non-contaminated sample (C = 0 g/l) as reference, we noticed, that its equilibrium water content was reached for less RH when concrete was contaminated, especially for important concentrations (C = 120 g/l). Indeed, the equilibrium water content of BFSC60, without chloride contamination, was of 1.4% when RH = 73% (Fig. 8). This water content was reached at RH = 60%, RH = 48% and RH = 30% for concrete specimens contaminated, respectively, with chloride solution of 30, 60 and 120 g/l of NaCl. If the trend is in agreement with the results of Bonnet and Perrin [41], the drop of relative humidity corresponding to the water equilibrium content does not follow any law. Indeed, Bonnet and Perrin [41] have determined shift coefficients depending on chloride concentration of used contaminating solution for tested mortars. This coefficient is ≈0.94 for a solution of 30 g/l of NaCl. In our case, we have used crushed concrete, so the presence of coarse aggregates could modify the water vapour adsorption of samples in comparison to mortars' ones.

This new result highlights the significant effect of chloride–matrix interaction on water vapour sorption. Indeed, in real conditions, when concretes are exposed to salt water, chloride binding occurs in the same time that water vapour adsorption, which could accelerate the process of chloride absorption and then the chloride content. Thus, all transfer models presented in the literature and based on water vapour isotherms adsorption of non-contaminated concretes, could under-estimate chloride ingress in concrete and then corrosion risk of steel.

4.2.2.3. Modeling of water vapour adsorption isotherms. Many models could be used to describe sorption phenomenon [25]. Some of them concern only one part of the curve (w versus RH). GAB model, governed by Eq. (3) [42] (cited in [41]), allows a complete representation of water vapour adsorption isotherm.

$$w = \frac{\mathrm{RH}}{a\mathrm{RH}^2 + b\mathrm{RH} + c} \times \frac{1}{(1-\mathrm{RH})^d} \tag{3}$$

where w and RH are respectively water content (%) and relative humidity (%); a, b, c and d are numerical parameters.

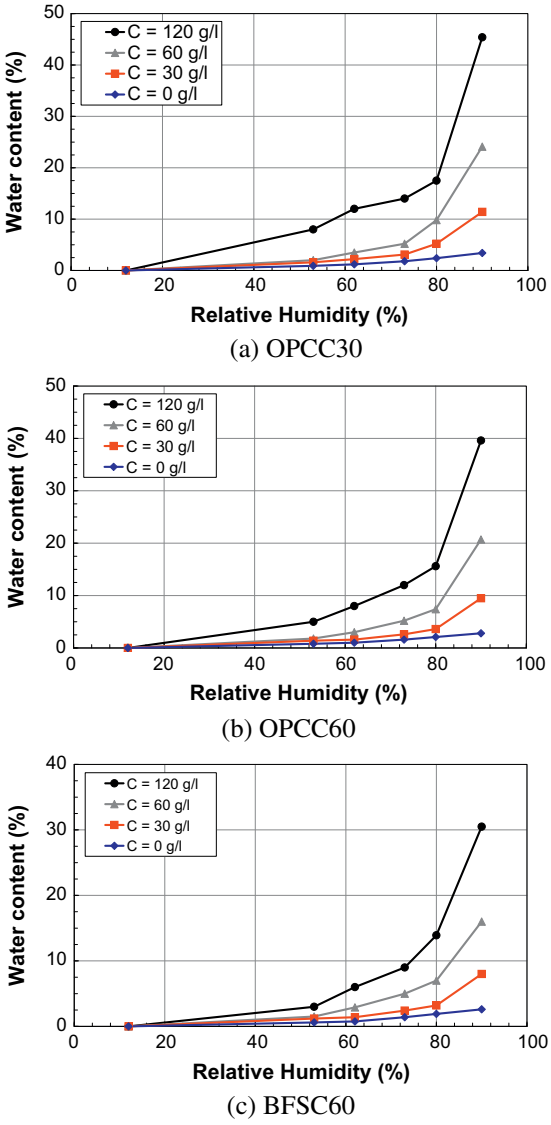

Fig. 10. Water vapour absorption isotherms of: (a) OPCC30, (b) OPCC60 and (c) BFSC60 for different external chloride concentrations.

In order to show the influence of chloride/concrete interactions on adsorption isotherms, we compared the results of tests on non-contaminated (C = 0 g/l) and contaminated concretes with chloride solution of 30 g/l (Fig. 11). The first concentration (C = 0 g/l) is the common concentration for all previous studies, on adsorption isotherms. The second one (30 g/l), have been chosen to simulate the real state of reinforced concrete structure in marine environment.

Experimental curve of water content versus relative humidity, for non-contaminated concrete is fitting using GAB model and the numerical equation was then used in transfer models to estimate chloride ingress. As shown in Fig. 11 and Table 5, the numerical parameters for GAB model could change strongly when we took into account chloride/matrix interaction. This would have a great influence on the numerical estimated transfer parameters of concrete and then its corrosion risk and durability.

4.3. Chloride transport

In this study, only total chloride profiles were determined and analysed at the end of each contamination's duration. To get clear figures, only chloride profiles of 75% and 90% RH, which are the

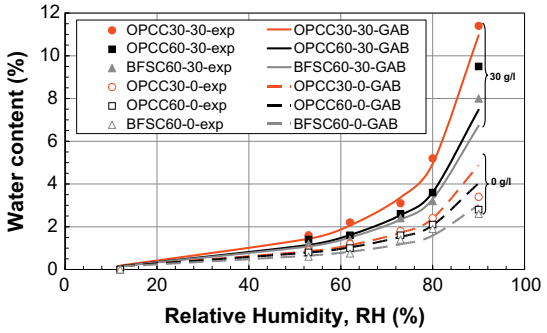

Fig. 11. Comparison of experimental (exp) and numerical (GAB) water vapour adsorption isotherms for C = 0 g/l and C = 30 g/l and for different concretes.

Table 5
Numerical coefficients of GAB model for C = 0 g/l and C = 30 g/l.

	C = 0 g/l			C = 30 g/l		
	OPCC30	OPCC60	BFSC60	OPCC30	OPCC60	BFSC60
a	10	15	55	1	2	4
b	85	100	125	5	10	20
c	80	75	80	75	85	85
d	0.95	0.9	0.9	0.99	0.9	0.9

most representative for marine structures in North Atlantic area, have been plotted in Fig. 12a–c.

The shapes are similar for all curves. An increasing of chloride concentration is noticed in the skin layer (first millimetres) before getting a maximum content. Then chloride concentration decreases with a regular shape (diffusion process) within concretes except for OPCC30. This increasing–decreasing shape is due to the outward convection at the concrete surface.

To determine the apparent diffusion coefficient D_a, the decreasing part of the experimental data is fitting with the second Fick's law (§ 3.6.4) by adjusting the surface content (C_s) and D_a [33]. These parameters are summarised in Tables 6–8, for all concretes and exposure times in different relative humidity ambiances.

4.3.1. Effect of time exposure

As expected, the chloride content and the maximum penetration depth increase as the number of cycles increases, and the chloride concentration decreases along the depth from the exposed surface to the concrete's heart.

Fig. 13 shows the chloride coefficient evolution versus exposure time for OPCC60 and BFSC60. Chloride diffusion coefficients are not drawn for OPCC30: the application of Eq. (2) could be discussed for this concrete. Indeed chloride contents are very important and the profiles are almost constant for 60 cycles (no decreasing). In this case the fitting is not appropriate as the medium is not semi infinite (for semi infinite medium: $c = 0$ for a depth of 50 mm).

As shown in Fig. 13, the chloride diffusion coefficient versus exposure time presents an exponential decreasing, for both presented concretes and for all RH. For first days of salt exposure, chloride gradient between external solution and concrete is very high (30 g/l of NaCl), which accelerates chloride diffusion by concentration gradient. Otherwise, concrete pores are less saturated for first cycles and the capillary absorption of salt solution is great. As the time exposure increases, pores' saturation increases gradually and chloride gradient decreases which induces lowest chloride diffusion coefficient. This coefficient decreases about five times for both concretes and for three RH, when the exposure time increases from 1 to 30 days (2–60 cycles).

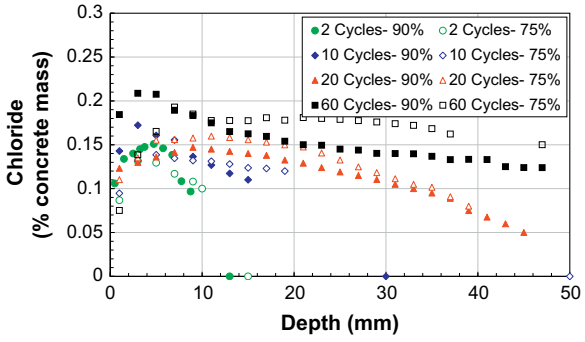

(a) OPCC30

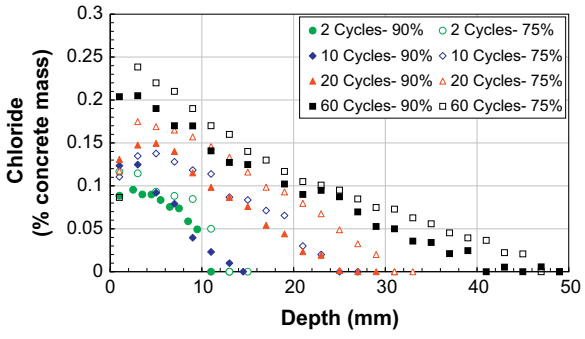

(b) OPCC60

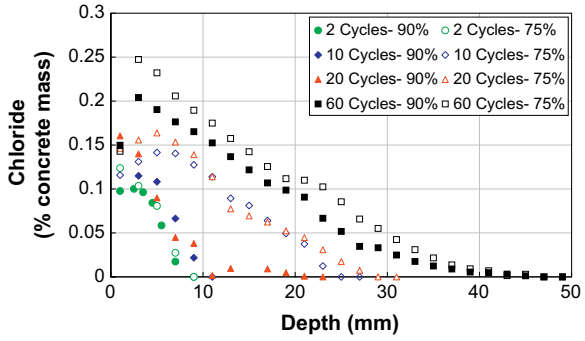

(c) BFSC60

Fig. 12. Total chloride profiles measured at RH = 90% and RH = 75%, after 2, 10, 20 and 60 cycles, on (a) OPCC30, (b) OPCC60 and (c) BFSC60.

4.3.2. Effect of RH on chloride transport

Moreover as humidity is decreasing, the chloride concentration and maximum penetration depth are increasing, which proves that diffusion due to concentration gradient is not the only mechanism governing chloride transport in unsaturated concrete. Indeed, the moisture concrete gradient and the capillary absorption could change the trend of chloride profiles. The chlorides penetrate into concrete during wetting period by following the liquid phase, which penetrates by liquid pressure gradient. In the drying period only water evaporates from the concrete surface and the dissolved salts are crystallised on pores surface. Thus the chloride content in concrete continuously increases. This phenomenon is more pronounced for lowest humidities because liquid penetrates more, by capillary absorption, into concrete when its moisture content is lower. The basic trend of our curves agrees with the coupling effect of moisture and chloride penetration predicted by the numerical model of Ababneh et al. [12] which showed a greater chloride penetration depth and concentration in concrete with 50% initial relative humidity (maximal penetration depth = 2.75 cm) compared to fully saturated concrete (maximal penetration depth = 2 cm). In

Table 6
Total chloride profiles parameters for OPCC30.

Time (days)	Time (cycles)	HR = 50%		HR = 75%		HR = 90%	
		C_s	D_a	Cs	D_a	Cs	D_a
1	2	0.13	8.3	0.129	75	0.148	30
5	10	0.181	30	0.169	20	0.168	12
10	20	0.136	70	0.11	55	0.173	11
30	60	0.16	90	0.21	90	0.184	10

C_s: chloride content at the surface (%); D_a: apparent diffusion coefficient (10^{-10} m^2/s).

Table 7
Total chloride profiles parameters for OPCC60.

Time (days)	Time (cycles)	HR = 50%		HR = 75%		HR = 90%	
		C_s	D_a	Cs	D_a	Cs	D_a
1	2	0.145	12	0.12	8.5	0.107	7.5
5	10	0.15	10	0.16	7	0.123	5
10	20	0.179	9	0.22	4	0.144	3
30	60	0.19	2.5	0.24	1.5	0.205	1.4

C_s: chloride content at the surface (%); D_a: apparent diffusion coefficient (10^{-10} m^2/s).

Table 8
Total chloride profiles parameters for BFSC60.

Time (days)	Time (cycles)	HR = 50%		HR = 75%		HR = 90%	
		C_s	D_a	Cs	D_a	Cs	D_a
1	2	0.14	11	0.107	3.5	0.085	1.5
5	10	0.13	9.7	0.165	3	0.11	0.8
10	20	0.175	8.5	0.18	2.5	0.145	0.4
30	60	0.22	2	0.247	1.22	0.204	0.35

C_s: chloride content at the surface (%); D_a: apparent diffusion coefficient (10^{-10} m^2/s).

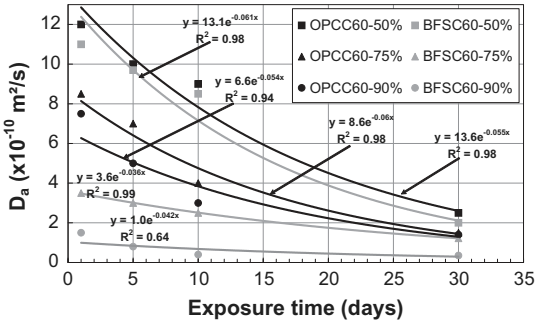

Fig. 13. Apparent diffusion coefficient versus exposure time.

2010, Bermudez and Alaejos [17] compared experimental and numerical profiles of completely dried and saturated concretes. They measured that chloride content decreases two times in first millimetres when concrete samples were completely saturated.

For lowest relative humidities, concrete pores are less saturated and the moisture gradient is higher. So the pressure gradient in concrete is higher and the capillary absorption of salty water increases significantly: the chloride concentration and penetration depth and then the chloride diffusion coefficient are also increasing.

As shown in Table 9, after 1 month of drying wetting cycles (60 cycles), chloride diffusion coefficient of BFSC60 increases 3.5 times when relative humidity decreases from 90% to 75% and 5.7 times when it decreases to 50%. These results agree with the trend shown by Battacharjee and Nagesh [9]. These researchers compared completely dried and saturated concrete specimens, exposed continuously to salt solution. They measured that chloride

Table 9
Effect of RH on apparent chloride diffusion coefficient.

Concrete	$D_{a,ref}$ (for RH = 90%)	D_a (RH = 75)/$D_{a,ref}$	D_a (RH = 50)/$D_{a,ref}$
OPCC30	10	9	9
OPCC60	1.4	1.07	1.8
BFSC60	0.35	3.5	5.7

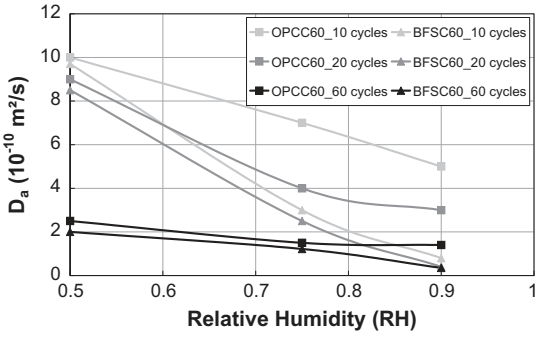

Fig. 14. Apparent diffusion coefficient versus Relative Humidity.

diffusion coefficient is 26 times more important in the first case for a chloride concentration of about 30 g/l.

Research results show the drastic dependency of chloride diffusion coefficient to RH. A relationship between chloride diffusion coefficient and relative humidity (Fig. 14, Table 10) has been established for OPCC60 and BFSC60 for 2, 10, 20 and 60 cycles.

4.3.3. Effect of water-to-binder ratio

The chloride concentration peaks are more pronounced and closer to the surface in the concrete with W/B = 0.48 (Fig. 12). In fact, a lower diffusion coefficient causes chloride accumulation in the superficial layer.

In contact with air, the skin layer of concrete exhibits continuously alternating moisture content, this could limit the chloride content in exposed surface. Such effect was more important for W/B = 0.7 concrete, especially for lowest humidity, because of its important porosity (Table 3).

As shown in Fig. 15, concrete with the highest W/B is more affected by moisture fluctuations and a decreasing of its moisture content from 90% to 75% increased by nine times its apparent diffusion coefficient. Its porosity is higher and the connectivity of the pore system is also increased, which results in an amplification of capillary absorption and a reduction in the resistance of the penetration moisture and chloride ions. As shown in Table 11, the decreasing of W/B from 0.7 to 0.48 induces a decreasing of 36, 60 and 7 times of apparent chloride diffusion coefficient for 50%, 75% and 90% of RH, respectively. This could be explained by the evolution of concrete porosity, as shown previously in Table 3.

Table 10
Correlation between chloride diffusion coefficient and RH.

Concrete	Exposure time (cycles)	Equation	Correlation coefficient
OPCC60	2	$D_a = -7.82\text{Ln(HR)} + 6.5$	0.99
	10	$D_a = -8.322\text{Ln(HR)} + 4.32$	0.99
	20	$D_a = -10.562\text{Ln(HR)} + 1.509$	0.97
	60	$D_a = -1.97\text{Ln(HR)} + 1.086$	0.95
BFSC60	2	$D_a = -16.55\text{Ln(HR)} - 0.66$	0.99
	10	$D_a = -15.37\text{Ln(HR)} - 1.065$	0.99
	20	$D_a = -13.95\text{Ln(HR)} - 1.25$	0.99
	60	$D_a = -2.62\text{Ln(HR)} + 0.227$	0.94

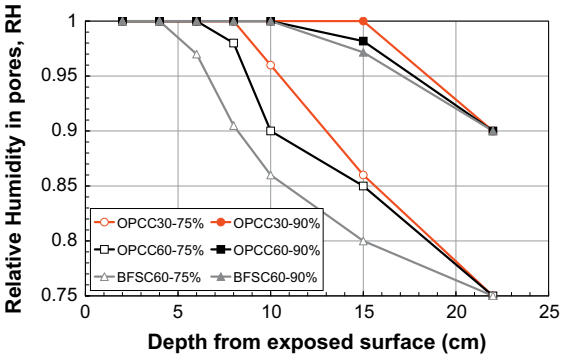

Fig. 15. RH profiles after 60 cycles.

Table 11
Effect of W/B on apparent chloride diffusion coefficient.

RH (%)	$D_{a,OPCC30}/D_{a,OPCC60}$
50	36
75	60
90	7

Fig. 15 demonstrates clearly the important value of relative humidity in OPCC30 after 60 cycles. This figure highlights the faster humidity diffusion transport in concrete with the highest W/B. The results agree with numerical predictions of Ababneh et al. [12]. They measured diffusion coefficient as a function of water-to-cement ratio; the higher the W/C, the higher the humidity diffusion coefficient.

Humidity diffusion will induce faster chloride solution sucking in porous concrete and then more chloride content. A decreasing of four times of chloride diffusion coefficient, has been numerically predicted by Ababneh et al. [12] when W/C decreases from 0.5 to 0.6 and for RH = 90%. In 2010, Bermudez and Alaejos [17] predicted the same trend.

4.3.4. Effect of slag's addition

Fig. 12 shows that concrete with slag addition presented the lowest chloride ingress and then the lowest apparent diffusion coefficient. This could be explained by the denser structure of this type of concrete and its high content of aluminates, which increases its binding capacity. Indeed the addition of slag reduces the porosity of concrete, increasing its strength and performing its capacity to resist to chloride ingress [43].

As shown in Table 12, the substitution of 30% of cement by slag decreases chloride diffusion by 1.3, 1.2 and 4 times for RH of 50%, 75% and 90%, respectively. In agreement with our results, Michael et al. [44] have shown, for W/C = 0.4 concrete and after 25 years seawater exposure time, that the chloride diffusivity could be reduced by approximately 6 and 14 times, when the cement is replaced by 25% and 45% of slag, respectively.

4.3.5. Effect of saturation rate of concrete

Fig. 16 shows a comparison of chloride profiles of different studied concretes, subjected to wetting/drying cycles (WD) at 75% of RH (empty symbol) and continuously (C) in contact with chloride solution of 30 g/l (full symbol) (NT BUILD 443 [33]) for 1 month. This result highlights the aggressiveness of tidal zone where drying diminishes the internal relative humidity of concrete and increases the chloride concentration on the surface and then increases the chloride ingress by capillary absorption.

Table 12
Effect of slag on apparent chloride diffusion coefficient.

RH (%)	$D_{a,OPCC60}/D_{a,BFSC60}$
50	1.3
75	1.2
90	4

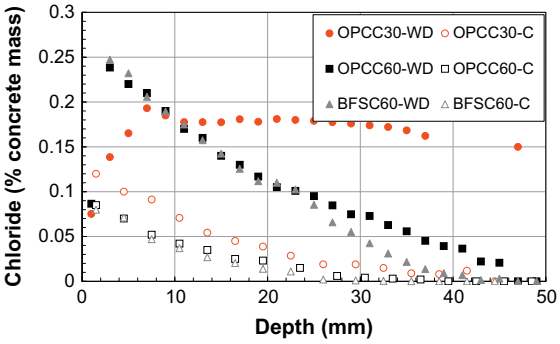

Fig. 16. Comparison of chloride profiles of different concretes exposed to NaCl wetting–drying cycles (WD) and continuously (C) for 1 month.

Besides the shape's difference, chloride concentrations are very different for both kinds of exposure. In fact, for cyclic movement, the skin layers of concrete are dried and chloride concentrations are low (for the first millimetres). For the same depth, of 1 cm, chloride concentrations are four times more important for drying/wetting cycles. This result is of great interest in engineering: in tidal zone, where coupled processes govern chloride transport, chloride ingress is faster. As it could be seen, in non-saturated structures, it is not only oxygen diffusion which accelerates corrosion but also the rapid reaching of critical chloride concentration, due to coupled transport phenomenon.

5. Conclusions and further research

This study investigates chloride penetration in non-saturated concrete, subjected to wetting/drying cycles. The effects of coupling moisture and chloride transfer in concrete submitted to drying–wetting cycles have been experimentally analysed.

The following main conclusions can be drawn:

5.1. Metrological development

A new test method to control the initial moisture content of samples has been presented. Capacitive probes have been used for this aim.

A new experimental setup, allowing an automatic application of drying–wetting cycles, in controlled environmental conditions, has been developed. The relative humidity profiles could be measured, during the test, using capacitive probes.

5.2. Experimental results

Various experimental results have been presented in this paper. A database useful for further researches is thus available, in particular in physical models, coupling chloride and moisture transport:

The partial substitution of cement by slag decreases the porosity of concrete and ameliorates its mechanical and transfer properties. The fineness of slag confers to concrete a great chloride resistance.

The chloride binding has a drastic influence on water vapour sorption phenomenon. Results show clearly the inadequacy, which can arise between the water vapour adsorption isotherms, usually used (with C = 0 g/l) in models and those actually measured. Indeed, equilibrium water content of tested concretes, for RH = 73%, increases ≈2 times when external chloride solution concentration increases from 0 to 30 g/l.

The decreasing of RH diminishes the moisture content of concrete and preserves its pores less saturated (Fig. 15). Therefore, chloride ingress by capillary absorption was accelerated. This interesting result was greatly illustrated in Fig. 16, which shows the significant difference between chloride content of saturated and non-saturated concretes. In the first one, pure diffusion operates solely. In non-saturated materials, chloride content due to capillary absorption and convection represent 75% (until 20 mm) of total chloride content of concrete. The relationship, established between chloride diffusion coefficient (D_a) and RH, confirms this trend.

The increasing of water-to-binder-ratio increases concrete porosity and reduces its binding capacity (by reducing cement content), which induces greater chloride depth and concentration. However, the addition of slag seems to improve the resistance of concrete to chloride diffusion, by increasing its binding capacity and then by decreasing its apparent chloride diffusion coefficient. This is due to the dense structure of slag-blended concrete caused by the relatively large amount of C–S–H formed in the products.

Finally, we hope that this work will lead to the validation of existing models, the development and the validation of new simulation tool of a more detailed understanding of the mechanisms of chloride transport in non-saturated cementitious materials. Therefore, it should be pointed out that further research should be useful in order to develop a physical model coupling moisture, chloride and drying. To achieve this aim, our actual work gives some results, which could be used as input and/or output data for this physical model.

Acknowledgements

The technical help of M. Roger Coué in experimental setup development is gratefully acknowledged. The authors acknowledge also financial support of national Project 'Maintenance and Repair of concrete coastal structures: risk-based Optimization' (MAREO Project) and international Project 'Durable Transport Infrastructures in Atlantic Area – Network' (duratiNET Project).

References

[1] Hwan-Oh B, Yup Jang S. Effects of material and environmental parameters on chloride penetration profiles in concrete structures. Cem Concr Res 2007;37(1):47–53.
[2] Mehta PK. Concrete: structure, properties and materials. Ed Prentice-Hall; 1986. p. 105–169.
[3] Khelidj A, Loukili A, Bastian G. Experimental study of the hydro-chemical coupling inside maturing concretes: effect on various types of shrinkage. Mater Struct 1998;31(9):588–94.
[4] Nielsen EP, Geiker MR. Chloride diffusion in partially saturated cementitious material. Cem Concr Res 2003;33(1):133–8.
[5] Hong K, Hooton RD. Effects of cyclic chloride exposure on penetration of concrete cover. Cem Concr Res 1999;29(9):1379–86.
[6] Conciatori D, Sadouki H, Brühwiler E. Capillary suction and diffusion model for chloride ingress into concrete. Cem Concr Res 2008;38(12):1401–8.
[7] Abdul-Hamid J, Mesfer M. Use of polypropylene fibers to enhance deterioration resistance of concrete surface skin subjected to cyclic wet/dry seawater exposure. Mater J 1990;87(4):363–70.
[8] Saetta A, Scotta R, Vitaliani R. Analysis of chloride diffusion into partially saturated concrete. ACI Mater J 1999;90(5):441–51.
[9] Nagesh M, Bhattacharjee B. Modeling of chloride diffusion in concrete and determination of diffusion coefficients. Mater J 1998;95(2):113–20.
[10] Maekawa K, Ishida T. Modeling of structural performances under coupled environmental and weather actions. Mater Struct 2002;35(10):591–602.
[11] Marchand J, Samson E, Maltais Y, Lee RJ, Sahu S. Predicting the performance of concrete structures exposed to chemically aggressive environmental-field validation. Mater Struct 2002;35(10):623–31.
[12] Ababneh A, Benboudjema F, Xi Y. Chloride penetration in nonsaturated concrete. J Mater Civil Eng, ASCE 2003;15(2):183–91.
[13] Samson E, Marchand J, Snyder K, Beaudoin J. Modeling ion and fluid transport in unsaturated cement systems in isothermal conditions. Cem Concr Res 2005;35(1):141–53.
[14] Meijers S, Bijen J, Borst R, Fraiij A. Computational results of a model for chloride ingress in concrete including convection, drying- wetting cycles and carbonation. Mater Struct 2005;38(2):145–54.
[15] Nguyen T, Petkovic J, Dangla P, Baroghel-Bouny V. Modelling of coupled ion and moisture transport in porous building materials. Construct Build Mater 2008;22(11):2185–95.
[16] Iqbal P, Ishida T. Modeling of chloride transport coupled with enhanced moisture conductivity in concrete exposed to marine environment. Cem Concr Res 2009;39(4):329–39.
[17] Bermudez MA, Alaejos P. Models for chloride diffusion coefficients of concretes in tidal zone. Mater J 2010;107(1):3–11.
[18] Bastidas- Arteaga E, Chateauneuf A, Sanchez- Silva M, Bressolette P, Schoefs F. A comprehensive probabilistic model of chloride ingress in unsaturated concrete. Eng Struct 2011;33(3):720–30.
[19] Climent M, De Vera J, Lopez J, Viqueira E, Andrade C. A test method for measuring chloride coefficients trough nonsaturated concrete, Part I. The instantaneous plane source diffusion case. Cem Concr Res 2002;32(7):1113–23.
[20] Taheri-Motlagh A. Durability of reinforced concrete structures in aggressive marine environment. PhD dissertion. Delft University of technology; 1998.
[21] McCarter W, Chrisp T, Butler A, Basheer P. Near-surface sensors for condition monitoring of cover-zone concrete. Construct Build Mater 2001;15(2–3):115–24.
[22] Norris A, Saafi M, Romine P. Temperature and moisture monitoring in concrete structures using embedded nanotechnology/microelectromechanical systems (MEMS) sensors. Construct Build Mater 2008;22(2):111–20.
[23] European Standard NF EN 206-1; 2005.
[24] Picandet V, Khelidj A, Bastian G. Effect of axial compressive damage on gas permeability of ordinary and high-performance concrete. Cem Concr Res 2001;31(11):1525–32.
[25] Ben Fraj A. Transfer in non-saturated concretes: influence of slag and mechanical damage. PhD thesis of Nantes' University, France; 2009 ((in French)).
[26] Kollek JJ. The determination of the permeability of concrete to oxygen by the cembureau method – a recommendation. Mater Struct 1989;22(3):225–30.
[27] Andrade C. Calculation of chloride diffusion coefficients in concrete from ionic migration measurements. Cem Concr Res 1993;23(3):724–42.
[28] AFPC-AFREM. Recommended methods for measuring durability parameters. France; 1997 (in French).
[29] Tang L, Nilsson LO. Chloride binding capacity and binding isotherms of OPC pastes and mortar. Cem Concr Res 1993;23(2):247–53.
[30] Baroghel-Bouny V. Water vapour sorption experiments on hardened cementitious materials, Part I. Essential tool for analysis of hygral behaviour and its relation to pore structure. Cem Concr Res 2007;37(3):414–37.
[31] Baroghel-Bouny V. Water vapour sorption experiments on hardened cementitious materials, Part II. Essential tool for assessment of transport properties and for durability prediction. Cem Concr Res 2007;37(3):438–54.
[32] Crank J. The Mathematics of Diffusion, 2nd ed. UK: Oxford Science Publications; 1975.
[33] Vichot A, Ollivier JP. Durability of concretes, 2nd ed. ENPC; 2008 (in French).
[34] Hirao H, Yamada K, Takahashi H, Zibara H. Chloride binding of cement estimated by binding isotherms of hydrates. J Adv Concr Technol 2005;3(1):77–84.
[35] Arya C, Buenfeld NR, Newman JB. Factors influencing chloride binding in concrete. Cem Concr Res 1990;20(2):291–300.
[36] Dhir RK, El-Mohr MAK, Deyer TD. Developing chloride resisting concrete using PFA. Cem Concr Res 1997;27(11):1633–9.
[37] Xu Y. The influence of sulphates on chloride binding and pore solution chemistry. Cem Concr Res 1997;27(12):1841–50.
[38] Yuan Q, Caijun S, De Schutter G, Audenaert K, Deng D. Chloride binding of cement-based materials subjected to external chloride environment – a review. Construct Build Mater 2009;23(1):1–13.
[39] Truc O. Prediction of chloride penetration into saturated concrete – multispecies approach. PhD thesis of Chalmers University of Technology; 2000.
[40] Baroghel-Bouny V, Mainguy M, Lassabatere T, Coussy O. Characterization and identification of equilibrium and transfer moisture properties for ordinary and high-performance cementitious materials. Cem Concr Res 1999;29(8):1225–38.
[41] Bonnet S, Perrin B. Influence of chloride ions on equilibrium properties of different mortars. Mater Struct 1999;32(7):492–9 (in French).
[42] Miquel A. Experimental determination of hydrous properties of building materials: contribution of development and validation of new techniques. PhD thesis of Paris XII University; 1997 (in French).
[43] Guneyisi E, Gesoglu M. A study on durability properties of high-performance concretes incorporating high replacement levels of slag. Mater Struct 2008;41(3):479–93.
[44] Michael DAT, Allan S, Ted B, Alain B, Donna D. Performance of slag concrete in marine environment. Mater J 2008;105(6):628–34.